

1 Global hotspots for soil nature conservation

2 Carlos A. Guerra^{1,2,4}, Miguel Berdugo⁷, David J. Eldridge³, Nico Eisenhauer^{1,4}, Brajesh K. Singh^{5,6},
3 Haiying Cui^{8,9}, Sebastian Abades¹⁰, Fernando D. Alfaro^{10,11}, Adebola R. Bamigboye¹², Felipe Bastida¹³,
4 José L. Blanco-Pastor¹⁴, Asunción de los Ríos¹⁵, Jorge Durán^{16,37}, Tine Grebenc¹⁷, Javier G. Illán¹⁸, Yu-
5 Rong Liu¹⁹, Thulani P. Makhalanyane²⁰, Steven Mamet²¹, Marco A. Molina-Montenegro^{22,23}, José L.
6 Moreno¹³, Arpan Mukherjee²⁴, Tina U. Nahberger¹⁷, Gabriel F. Peñaloza-Bojacá²⁵, César Plaza²⁶,
7 Sergio Picó²⁷, Jay Prakash Verma²⁴, Ana Rey¹⁵, Alexandra Rodríguez¹⁶, Leho Tedersoo^{33,34}, Alberto L.
8 Teixido²⁸, Cristian Torres-Díaz²⁹, Pankaj Trivedi³⁰, Juntao Wang⁵, Ling Wang⁸, Jianyong Wang⁸, Eli
9 Zaady³¹, Xiaobing Zhou³², Xin-Quan Zhou¹⁹, Manuel Delgado-Baquerizo^{35,36}

10 ¹ German Centre for Integrative Biodiversity Research (iDiv) Halle-Jena-Leipzig, Leipzig, Germany

11 ² Institute of Biology, Martin Luther University Halle Wittenberg, Am Kirchtor 1, 06108 Halle(Saale), Germany

12 ³ Centre for Ecosystem Science, School of Biological, Earth and Environmental Sciences, University of NSW,
13 Sydney, 2052 Australia

14 ⁴ Institute of Biology, Leipzig University, Puschstrasse 4, 04103 Leipzig, Germany

15 ⁵ Hawkesbury Institute for the Environment, Western Sydney University, Penrith, New South Wales 2751, Australia

16 ⁶ Global Centre for Land-Based Innovation, Western Sydney University, Penrith, NSW 2751, Australia

17 ⁷ Institute of Integrative Biology, Department of Environment Systems Science, ETH Zürich, 8092 Zürich,
18 Switzerland

19 ⁸ Institute of Grassland Science, School of Life Science, Northeast Normal University, Key Laboratory of Vegetation
20 Ecology of the Ministry of Education, Jilin Songnen Grassland Ecosystem National Observation and Research
21 Station, Changchun, China

22 ⁹ Departamento de Sistemas Físicos, Químicos y Naturales, Universidad Pablo de Olavide, Sevilla, Spain

23 ¹⁰ GEMA Center for Genomics, Ecology & Environment, Faculty of Interdisciplinary Studies, Universidad Mayor,
24 Camino La Pirámide 5750, Huechuraba, Santiago, Chile

25 ¹¹ Instituto de Ecología & Biodiversidad (IEB), Santiago, Chile

26 ¹² Natural History Museum, Obafemi Awolowo University, Ile-Ife, Nigeria

27 ¹³ CEBAS-CSIC, Campus Universitario de Espinardo, 30100, Murcia, Spain

28 ¹⁴ Department of Plant Biology and Ecology, University of Seville. Avda. Reina Mercedes 6. ES-41012 Seville,
29 Spain

30 ¹⁵ Museo Nacional de Ciencias Naturales. Consejo Superior de Investigaciones Científicas, Serrano 115 bis,
31 28006, Madrid, Spain.

32 ¹⁶ University of Coimbra, Centre for Functional Ecology, Department of Life Sciences, Calçada Martim de Freitas,
33 3000-456 Coimbra, Portugal

34 ¹⁷ Slovenian Forestry Institute, Večna pot 2, SI-1000 Ljubljana, Slovenia

35 ¹⁸ Department of Entomology. College of Agricultural, Human, and Natural Resource Sciences. Washington State
36 University. Pullman, WA, 99164. USA

37 ¹⁹ College of Resources and Environment, Huazhong Agricultural University, Wuhan 430070, China

38 ²⁰ Department of Biochemistry, Genetics and Microbiology, University of Pretoria, South Africa

39 ²¹ College of Agriculture and Bioresources Department of Soil Science. University of Saskatchewan, Saskatoon,
40 SK S7N 5A8. Canada

41 ²² Laboratorio de Ecología Integrativa, Instituto de Ciencias Biológicas, Universidad de Talca, Talca, Chile

42 ²³ CEAZA, Universidad Católica del Norte, Coquimbo, Chile

43 ²⁴ Institute of Environment and Sustainable Development, Banaras Hindu University, Varanasi-221005, Uttar
44 Pradesh, India

45 ²⁵ Departamento de Botânica, Universidade Federal de Minas Gerais, Belo Horizonte, MG, Brazil

46 ²⁶ Instituto de Ciencias Agrarias, Consejo Superior de Investigaciones Científicas, Madrid, Spain

47 ²⁷ Departamento de Biología, Instituto Universitario de Investigación Marina (INMAR), Universidad de Cádiz,
48 11510, Puerto Real, Spain

49 ²⁸ Departamento de Botânica e Ecologia, Instituto de Biociências, Universidade Federal de Mato Grosso, Av.
50 Fernando Corrêa, 2367, Boa Esperança, Cuiabá, 78060-900, MT, Brazil

51 ²⁹ Grupo de Investigación en Biodiversidad y Cambio Global (GI BCG), Departamento de Ciencias Básicas,
52 Universidad del Bío-Bío, Chillán, Chile

53 ³⁰ Microbiome Network and Department of Agricultural Biology, Colorado State University, Fort Collins, USA 80523

54 ³¹ Department of Natural Resources, Agricultural Research Organization, Institute of Plant Sciences, Gilat
55 Research Center, Mobile Post Negev, 8531100, Israel

56 ³² State Key Laboratory of Desert and Oasis Ecology, Xinjiang Institute of Ecology and Geography, Chinese
57 Academy of Sciences, Urumqi, China

58 ³³ Mycology and Microbiology Center, University of Tartu, 14a Ravila, 50411 Tartu, Estonia

59 ³⁴ College of Science, King Saud University, Riyadh, Saudi Arabia
60 ³⁵ Laboratorio de Biodiversidad y Funcionamiento Ecosistémico. Instituto de Recursos Naturales y Agrobiología de
61 Sevilla (IRNAS), CSIC, Av. Reina Mercedes 10, E-41012, Sevilla, Spain.
62 ³⁶ Unidad Asociada CSIC-UPO (BioFun). Universidad Pablo de Olavide, 41013 Sevilla, Spain.
63 ³⁷ Misión Biológica de Galicia, Consejo Superior de Investigaciones Científicas, 36143 Pontevedra, Spain

64

65 **Corresponding Authors:** Carlos A. Guerra (carlos.guerra@idiv.de); Manuel Delgado-
66 Baquerizo (m.delgado.baquerizo@csic.es)

67 **Abstract**

68 Soils are the foundation of all terrestrial ecosystems ¹. However, unlike for plants and animals,
69 a global assessment of the hotspots for soil nature conservation is still lacking ². This hampers
70 our ability to establish nature conservation priorities for the multiple dimensions supporting the
71 soil system: from soil biodiversity to ecosystem services. Here, we conducted a global field
72 survey including biodiversity (archaea, bacteria, fungi, protists, and invertebrates) and function
73 (critical for six ecosystem services) observations within 615 composite topsoil samples from a
74 standardized survey in all continents, to identify global hotspots for soil nature conservation.
75 We found that each of the different soil ecological dimensions (i.e., soil species richness [alpha
76 diversity, measured as ASVs], community dissimilarity, and ecosystem services) peaked in
77 contrasting regions of the planet, and were associated with different environmental factors.
78 Temperate ecosystems showed the highest species richness, while community dissimilarity
79 peaked in the tropics, and colder high-latitude ecosystems were identified as hotspots of
80 ecosystem services. These findings highlight the complexities of simultaneously protecting
81 multiple soil ecological dimensions. We further show that most of these hotspots are not
82 properly covered by protected areas (over 70%), and are vulnerable in the context of multiple
83 global change scenarios. This first global estimation of soil nature conservation priorities,
84 highlights the fundamental importance of accounting for the multidimensionality of soil
85 biodiversity and ecosystem services to conserve soils for future generations.

86 **Main text:**

87 Soils are essential to support terrestrial life on the planet ¹. They are home to diverse
88 assemblages of organisms across all major lineages of life from bacteria to invertebrates, and
89 provide multiple ecosystem services such as soil fertility, carbon (C) storage, waste
90 decomposition, pest control, and water retention ³⁻⁵ that are critical for food production and
91 human well-being ⁶⁻⁸. However, soils are also highly vulnerable to anthropogenic disturbances
92 such as climate change ^{9,10} and land use intensification (e.g., land-use change, pollution, and
93 erosion ^{11,12}). For an adequate conservation of soils, it is critical to consider and protect the

94 multiple ecological dimensions supported by soils, from their biodiversity to the different
95 ecosystem services they support. A first step in this direction is identifying the global ecological
96 hotspots for soil nature conservation ¹³ to inform and guide policymakers and conservation
97 managers on how to extend nature conservation to the world belowground. Concurrently,
98 establishing and negotiating adequate global nature conservation policies and priorities (e.g.,
99 the 2030 biodiversity targets ¹⁴) requires knowledge about the distribution of global
100 biodiversity, including identifying ecological hotspots ². While these ecological hotspots were
101 established decades ago for plants and animals, this critical information for soil biodiversity
102 and ecosystem services does not exist and is therefore absent from current biodiversity
103 assessments ¹⁵. Recent developments in ecological modeling and soil macroecology have
104 improved our understanding of the global distribution of multiple soil communities ¹⁶⁻²¹ and
105 their potential future trends ^{9,22}. These studies have found potential mismatches between
106 below- and aboveground biodiversity, suggesting that hotspots of plant diversity are poor
107 proxies of belowground diversity ²³ and, therefore, are unlikely to provide sufficient protection
108 for life belowground. While this may be true, plant species richness, like the one found in the
109 tropics, is known to increase the diversity in soil organic matter compounds and, therefore,
110 provide resources for a diverse soil microbiological community ²⁴. This also opens the question
111 to if the hotspots of different soil ecological dimensions (e.g., diversity, community
112 composition, functions) coincide in space and how these are affected by global change, with
113 recent studies pointing to diverging global patterns ²². Yet, many recent developments are
114 based on merged meta-analytical data, which are rarely measured using the same methods
115 or do not simultaneously consider multiple soil ecological dimensions in the same locations.
116 Unfortunately, we still lack globally standardized field surveys that explicitly consider the
117 ecological multidimensionality of soils that simultaneously capture information on multiple soil
118 taxonomic groups and ecosystem services, across a wide range of global environmental
119 conditions ²⁵. Closing these knowledge gaps is essential to inform the establishment of nature
120 conservation areas, steer management decisions, and set effective policy targets that address
121 the ecological conservation of soils.

122 Herein, we combined machine learning models with a standardized global field survey,
123 including 615 composite topsoil samples from all continents and climates (Supplementary
124 Fig.1) to estimate, for the first time, the extent, associated environmental factors, and climate
125 change vulnerabilities of the global hotspots of soil biodiversity and ecosystem services. Our
126 dataset is based on >11,000 individual standardized observations and including information
127 on 16 biodiversity and ecosystem service attributes (Methods; Supplementary Table 1). Our
128 study moved beyond the analysis of alpha diversity (here based on soil DNA amplicon
129 sequence variant, ASVs) and extended its scope to community dissimilarity (i.e., composition

130 heterogeneity, based on Jaccard distance from presence/absence data) of five soil groups of
131 organisms (archaea, bacteria, fungi, protists and invertebrates). Measuring the hotspots of
132 community dissimilarity and comparing them to the ones of alpha diversity allows us to identify
133 areas with high local diversity that, at the same time, contain unique communities. In addition,
134 to fully grasp the conservation potential of soil systems, soil functional properties related to six
135 key soil ecosystem services were assessed, including soil C storage (total soil organic C),
136 fertility (total nitrogen (N), phosphorus (P), potassium (K), and magnesium (Mg) contents;
137 terrestrial ecosystems in this study were not fertilized, and therefore, total nitrogen represents
138 the stocks of nitrogen in soil organic matter), organic matter decomposition (three enzymes
139 associated with starch and chitin degradation, and P mineralization), water retention (water-
140 holding capacity), pest control (inverse of the proportion of soil-borne fungal phytopathogens),
141 and mutualism (i.e. plant-mycorrhizal mutualism, an ecological relationship between plants
142 and fungi that is beneficial to both partners, assessed as the proportion of mycorrhizal fungi).
143 We acknowledge that our study does not cover the entire environmental spectra found on
144 Earth, but it represents a large portion of the environmental variability found in the planet
145 (Supplementary Fig. 1). Locations showing environmental conditions under-represented in our
146 study were excluded from our spatial analyses (Figs. 1-3).

147 Our analyses revealed that the assessed soil biodiversity and ecosystem services variables
148 are associated with contrasting environmental factors at the global scale (Extended Data Figs.
149 1 and 2). For example, while soil pH was the main factor associated with alpha diversity of soil
150 fungi and bacteria, soil organic matter (soil C and N contents) was positively associated with
151 the alpha diversity of protists and invertebrates (Extended Data Figs. 2 and 3), and elevation
152 was positively correlated with the alpha diversity of archaea. In the case of the assessed
153 ecosystem services, soil pH was positively associated with soil C content, water retention and
154 pest control, whereas, temperature was associated with organic matter decomposition and
155 fertility, and precipitation seasonality with mutualism (Extended Data Figs. 2 and 3). Although
156 many of these environmental associations are well-described in the literature (e.g., ^{26,27}), the
157 fact that different soil ecological dimensions could be predicted by contrasting environmental
158 factors was much less clear due to the lack of standardized global field surveys. These
159 contrasting associations and environmental drivers explain the different global distributions
160 found for each ecological dimension and reveal that important trade-offs may exist when
161 considering nature conservation of multi-faceted soil systems. To further visualize these trade-
162 offs, we used machine learning random forest spatial regression models together with
163 available current data and future projections for both climate and land-use change (2015-
164 2070), to predict the distribution of soil biodiversity and ecosystem services and assess their
165 major drivers according to multiple future scenarios (shared socioeconomic pathways (SSP);

166 SSP1: global sustainability, SSP3: regional rivalry, SSP4: inequality, and SSP5: fossil-fueled
167 development ²⁸). We standardized each of these spatial distributions and used a Getis-Ord
168 Gi* spatial clustering algorithm to obtain a representation of the global hotspots (clusters of
169 statistically high values) for the modelled distribution of each single biodiversity and ecosystem
170 service variable. These were then aggregated into each soil ecological dimension (Fig. 1A, B,
171 and C). To further strength our conclusions we performed a comparison across multiple
172 methods (Supplementary Figs. 7 and 10) and an uncertainty assessment for the spatial
173 predictions (Supplementary Figs. 5, 11, 12 and 13). A rationale supporting the spatial analysis
174 from our standardized survey, and explaining the limitations of our approach, is available in
175 the Method section.

176 Further, we showed that different ecological dimensions for soil conservation peak in different
177 regions of Earth (Fig. 1A, B, C). Model fitness (measured as overall training R²) varied between
178 0.855 and 0.914 for alpha diversity and community dissimilarity (Supplementary Table 5) and
179 between 0.801 and 0.936 for ecosystem services (Supplementary Table 6). Hotspots of alpha
180 diversity tend to have a wider distribution across the world, peaking in temperate and
181 Mediterranean regions, as well as in alpine tundra (overall occupying between 30.9%, for
182 archaea, and 42.4%, for bacteria, of the world). However, hotspots of community dissimilarity
183 occur around two contrasting global conditions, tropical systems and drylands (overall
184 occupying between 35.7%, for Archaea, and 43.0%, for Fungi, of the world). For Fungi, our
185 results were further compared and validated with an independent dataset (Supplementary Fig.
186 6). While higher alpha diversity may intuitively imply a direct decrease in dissimilarity, directly
187 varying in tandem, our results show that at the global scale this is not the case (Supplementary
188 Table 15). Archaea showed the highest proportion of shared hotspot areas with 19%, with all
189 other groups obtaining less than 8% (alpha diversity and community dissimilarity for the same
190 taxa; Supplementary Table 3). Our findings further suggest the existence of important trade-
191 offs in soil nature conservation priorities (Extended Data Fig. 3). For example, locations with
192 higher alpha diversity tend to be less dissimilar, and only a small proportion of locations were
193 found to support both high dissimilarity and alpha diversity (Fig. 1B). This proportion is smaller
194 for fungi (3.9%) and higher for Archaea (19.0%; Supplementary Table 2). Similarly, locations
195 with higher dissimilarity tend to have less soil C content, fertility, and higher proportion of plant
196 pathogens (Extended Data Fig. 3). Moreover, our global maps indicate that alpha diversity
197 (Fig. 1A), community dissimilarity (Fig. 1B), and ecosystem services (Fig. 1C) have their
198 hotspots in mostly contrasting regions of the planet, existing only in a few locations supporting
199 high levels of more than one of these dimensions (0.1% of the evaluated areas in the world;
200 based on Fig. 1). This contrasts with results found for other biodiversity groups like plants and
201 mammals ^{e.g., 29,30} and supports recent findings of a mismatch between soil biodiversity and

202 other taxonomic groups (Supplementary Table 13; ²³) While globally, tropical and arid systems
203 were mostly classified as locations with relatively low alpha diversity across taxa, these areas
204 are hotspots for soil community dissimilarity, supporting the most unique soil community
205 assemblies (Fig. 1B). In the case of bacteria, for example, locations with high pH support a
206 higher richness (e.g., in temperate systems); however, these are always similar organisms
207 which thrive in neutral-alkaline soils. This suggests that, while local diversity in tropical
208 systems may be low (e.g., as a consequence of acidic soils), these environmentally
209 contrasting areas of the globe may harbor unique communities, which in turn may result in
210 high gamma (regional) diversity. While this was already suggested in the past ^{16,22}, the present
211 study represents the first robust confirmation of this hypothesis.

212 Our results highlight the fact that preserving soils from a nature conservation perspective
213 requires a holistic approach that considers multiple soil ecological dimensions such as alpha
214 diversity, community dissimilarity, and ecosystem services in the context of a nature
215 conservation profile (Fig. 1D). Being able to position a given area within this soil nature
216 conservation profile allows to establish adequate conservation goals that effectively target the
217 preservation of soil communities and their effects on ecosystems ³¹. For example, an area that
218 falls into a community dissimilarity hotspot may focus on indicators and conservation goals to
219 track and prevent species losses, since these may be unique to its limits, while an area in an
220 ecosystem service hotspot may favor indicators that target ecosystem service supply. This
221 does not imply that conservation areas should not prioritize all soil ecological dimensions, but
222 rather that management strategies and conservation targets should be adjusted to the
223 ecological reality of each region and conservation area ². Moreover, while local approaches
224 are still needed to refine the local distribution of these hotspots ³², these results also suggest
225 that no particular region can protect all dimensions of soil conservation, making a further
226 argument for global cooperation and for establishing global soil nature conservation targets.

227 Given the contrasting regions supporting the highest biodiversity and services, identifying
228 which ecological dimension is the most relevant for the conservation of soil ecological
229 conditions is not a simple task. Some ecosystems depend on a high alpha diversity while
230 others do not need such high levels of alpha diversity to properly function but rely on more
231 dissimilar soil communities (Fig. 1D; ³³). Conversely, while for microbial communities ³⁴,
232 functional redundancy driven by community composition may be more important than alpha
233 diversity per se, in general terms, ecosystems with lower alpha diversity are likely to be more
234 sensitive to ecosystem change ³⁵ and for that, more targeted conservation actions are
235 required. Although it is known that soil organisms play a crucial role in ecosystem service
236 supply ³⁶, it is not clear that it is biodiversity per se that governs this entire process. For
237 example, some specific ecosystem services may depend on the presence of only a few

238 species, such as specific components of the soil nitrogen cycle ³⁷, while others are the result
239 of the activity of many species with high levels of redundancy, such as soil respiration ³⁸.
240 Therefore, we defined priority areas for soil nature conservation as areas supporting relatively
241 high levels of either soil biodiversity or ecosystem services. We were then able to identify key
242 regions of the planet surpassing high thresholds of either biodiversity or ecosystem service
243 provision - the hotspots for soil nature conservation - (Fig. 2). Considering the areas with the
244 highest accumulation of soil biodiversity hotspots (top 5% of areas), it is possible to identify
245 tropical systems and substantial areas in North America, in Northern Europe, and in Asia as
246 having high priority for nature conservation (Fig. 2A). These areas maximize different
247 dimensions of soil ecology and may thus require integrative strategies, not only from a nature
248 conservation perspective but also considering the socio-economic appropriation of
249 belowground systems. To this respect, it is striking that ~50% of these global nature
250 conservation priority areas are not under any form of nature conservation, and that only ~10%
251 correspond to areas fully preserved (Fig. 2B). Since these global soil nature conservation
252 priority areas are the areas with the highest nature conservation relevance and given that
253 currently soils do not have any specific nature conservation targets, this is a worrisome state
254 for the conservation of soil biodiversity worldwide ². This situation is also observed if we
255 consider other thresholds for the soil nature conservation potential (Fig. 2B). While soil
256 conservation may not be able to maximize all ecological dimensions at the same time, and
257 each region may have different specificities with specific research being required, a number
258 of actions may be considered. These include nature-based solutions in land management for
259 enhancing ecosystem services ³⁹, landscape-level actions like the preservation of permanent
260 forest and natural coverage in the surrounding of managed systems ⁴⁰, or nature-based
261 solutions focused on restoring or improving soil functional outputs ⁴¹. Our work provides key
262 information for regional and continental decision-makers to develop nature protection goals
263 that specifically target soil systems and biodiversity, including identifying areas with high
264 potential to establish soil-based nature conservation areas.

265 In the context of climate and land-use change, nature conservation areas and targets will need
266 to adapt to new conditions and also focus on mitigating potential impacts ⁴²⁻⁴⁴. Thus, focusing
267 on the global soil nature conservation priority areas (top 5%), we conducted an additional
268 analysis to predict the future changes in hotspots according to four shared socio-economic
269 pathways (Fig. 3; 2015-2070). Our projections highlight the fact that the soil nature
270 conservation hotspots will change as a result of climate and land-use change linked to
271 substantial declines in both alpha diversity and ecosystem services. Globally, across
272 scenarios, net differences between 2015-2070 range from 1.5% net gains in SSP3 and -12.2%
273 net losses in SSP5. In most cases these net changes actually hide substantial losses of

274 current soil nature conservation priority areas with 7.1% (SSP4) to 17.5% (SSP5) of current
275 areas being lost globally across different future scenarios (Supplementary Table 7). Our
276 results reveal that most of the net area losses are related to declines in ecosystem services,
277 particularly C stocks (average loss across scenarios = -6.8%) and mutualism (-3.8%) and litter
278 decomposition (-3.6%), and in alpha diversity of specific groups, particularly invertebrates (-
279 2.6%), fungi (-1.3%) and archaea (-1.1%). Our projections also show that new areas will
280 emerge as key areas for soil nature conservation across the world, corresponding to
281 expansions ranging from 5.3% in SSP5 (relative to the current area) to 9.5% in SSP3.
282 Surprisingly, scenarios that consider higher challenges for adaptation to climate change
283 motivated by higher regional income inequality and rivalry (SSP3 and SSP4; ⁴⁵), also show
284 the most positive effects for maintaining or expanding current nature conservation priorities
285 for soils, particularly in Africa and South America (Fig. 3). Overall, these positive effects are
286 mostly expected in the global south, with systematic negative effects in the global north across
287 scenarios. In fact, the only scenario where the global north has slight net gains (0.3-2.0%)
288 corresponds to the so-called “sustainability scenario” (SSP1). Nevertheless, in this scenario,
289 most of the rest of the world shows important net losses (-5.7% in Africa and -5.9% in Asia
290 Pacific) or just mild net gains (0.8% in South America) due to expected increases in global
291 economic development (Fig. 3). This is even more worrisome when considering recent reports
292 that show that 30% of the population across tropical countries are highly dependent on nature
293 ⁴⁶. Across all regions, the fossil-fueled economy scenario (SSP5) produces the strongest net
294 losses, with regions losing priority areas from -5.9%, for Asia-Pacific, to -31.8%, in the case of
295 North America (with most of these losses being driven by decreases in ecosystem services).
296 Furthermore, our results suggest that the current simplistic view on carbon-based targets
297 provides little protection for all soil ecological dimensions. In fact, the sustainability scenario
298 shows an overall global improvement in ecosystem services, with soil C leading these
299 improvements but with clear losses in alpha diversity. Together, these results indicate that
300 hotspots of soil biodiversity and ecosystem services are highly threatened by future climatic
301 and land-use changes, and stress the need for immediate protection of these locations. Our
302 findings also suggest that these hotspots might move in the future, with current sanctuaries of
303 soil biodiversity being subject to degradation.

304 In summary, based on the largest global standardized survey, including sixteen biodiversity
305 and ecosystem service variables, our work provides the first estimate of the global hotspots
306 for nature conservation of multiple soil ecological dimensions. Here, we identified critical
307 unique areas for the conservation of soil biodiversity and ecosystem services at the global
308 scale, with soil alpha diversity, dissimilarity, and services peaking in temperate, tropical, and
309 boreal regions, respectively. While recent literature highlights the need for extending nature

310 conservation to ensure global sustainability and the preservation of biodiversity ⁴⁷, it also
311 underlines that this increased protection requires context-based solutions ⁴⁸. By unveiling
312 important trade-offs in soil biodiversity and ecosystem services, we also highlighted that no
313 particular region of the world could simultaneously protect all soil ecological dimensions.
314 Therefore, the conservation of soil biodiversity and ecosystem services requires an integrated
315 approach that probably should not focus on locally maximizing all ecological dimensions at
316 the same time. Also, the fact that we found that these three ecological dimensions do not
317 necessarily match in terms of their spatial hotspots also showed the complexity of soil
318 ecosystems and highlighted the difficulty that land managers and policymakers face when
319 designing soil conservation measures. Nevertheless, we also showed that these nature
320 conservation priority areas are currently highly unprotected, with less than ~10% of these
321 locations under adequate conservation status. We acknowledge that our study is just a first
322 step towards understanding and mapping the global hotspots of soil nature conservation and
323 that high-resolution monitoring systems and multiple time periods are needed to better guide
324 regional conservation and policy options ². Still, our work suggests that current priority areas
325 of soil nature conservation are vulnerable to global change drivers in all future scenarios
326 considered, and stresses the need for immediate nature conservation targeting and protection
327 of these regions. This novel information and indicators should enable governments and
328 decision-makers to set soil nature conservation as a priority in the context of the 2030
329 Biodiversity Targets negotiations, paving the way for a more integrative view of nature.

330 **Author contributions**

331 C.A.G. and M.D-B. developed the original idea of the analyses presented in the manuscript.
332 M.D.-B. designed the field study and wrote the grant that funded the work. Field data were
333 collected by M.B., S.A., F.D.A., A.R.B., J.L.-B., A.d.I.R., J.D., T.G., J.G.I., Y-R.L., T.P.M., S.M.,
334 M.A.M-M., A.M., T.U.N., G.F.P-B., C.P., J.P.V., A.Re., A.R., A.L.T., C.T-D., P.T., L.W., J.W.,
335 E.Z., X.Z., X-Q. Z. and M.D-B. Lab analyses were done by M.D-B., H.C., F.B., J.L.M., S.P.
336 and L.T. Statistical analyses, mapping and ecological modelling was done by C.A.G., M.D-B.
337 and M.B.. Bioinformatic analyses were done by B.S. and J-T.W. The manuscript was written
338 by C.A.G. and M.D-B., edited by N.E. and D.E., with contributions from all co-authors.

339 **Data and code availability**

340 All the materials, raw data, and protocols used in the article are available upon request and
341 without restriction, and all data is be made publicly available in:
342 10.6084/m9.figshare.20221713

343 **Competing financial interests**

344 The authors declare no conflict of interest.

345 **Acknowledgements**

346 We thank all the researchers involved in the collection of field data. This project received
347 funding from the British Ecological Society (agreement nº LRA17\1193; MUSGONET). C.G.,
348 N.E. were funded by DFG– FZT 118, 202548816; C.G. was supported by FCT-PTDC/BIA-
349 CBI/2340/2020; M.D-B. was supported by RYC2018-025483-I, PID2020-115813RA-
350 I00\MCIN/AEI/10.13039/501100011033, and P20_00879. M.A.M-M and S.A. was funded by
351 FONDECYT 1181034 and ANID-PIA-Anillo INACH ACT192057. J.D. and A.R. acknowledge
352 support from IF/00950/2014, 2020.03670.CEECIND, SFRH/BDP/108913/2015, and
353 UIDB/04004/2020. Y-R.L. was supported by 2662019PY010 from the FRFCU. L.T. was
354 supported by the ESF grant PRG632. F.B. and J.M. were supported by i-LINK+2018
355 (LINKA20069) funded by CSIC. C.T.D. was supported by the Grupo de Biodiversidad &
356 Cambio Global UBB - GI 170509/EF. C.P. was supported by the EU H2020 grant agreement
357 No 101000224. H.C. was supported by NSFC32101335, FRFCU2412021QD014), and
358 CPSF2021M690589. JPV was supported by DST (DST/INT/SL/P-31/2021) SERB
359 (EEQ/2021/001083) and BHU-IoE (6031).

360

361 **References**

- 362 1. Bardgett, R. D. & van der Putten, W. H. Belowground biodiversity and ecosystem
363 functioning. *Nature* **515**, 505–511 (2014).
- 364 2. Guerra, C. A. *et al.* Tracking, targeting, and conserving soil biodiversity. *Science* **371**,
365 239–241 (2021).
- 366 3. Wall, D. H. *et al.* *Soil ecology and ecosystem services*. 406 (Oxford University Press,
367 2012).
- 368 4. Jansson, J. K. & Hofmockel, K. S. Soil microbiomes and climate change. *Nat. Rev.*
369 *Microbiol.* **18**, 35–46 (2020).
- 370 5. de Vries, F. T. *et al.* Soil food web properties explain ecosystem services across
371 European land use systems. *Proc. Natl. Acad. Sci. U. S. A.* **110**, 14296–14301 (2013).
- 372 6. Adhikari, K. & Hartemink, A. E. Linking soils to ecosystem services — A global review.
373 *Geoderma* **262**, 101–111 (2016).
- 374 7. Pereira, P., Bogunovic, I., Muñoz-Rojas, M. & Brevik, E. C. Soil ecosystem services,
375 sustainability, valuation and management. *Current Opinion in Environmental Science &*
376 *Health* **5**, 7–13 (2018).
- 377 8. Wall, D. H., Nielsen, U. N. & Six, J. Soil biodiversity and human health. *Nature* 1–8 (2015).
- 378 9. Delgado-Baquerizo, M. *et al.* The proportion of soil-borne pathogens increases with
379 warming at the global scale. *Nat. Clim. Chang.* **10**, 550–554 (2020).
- 380 10. Rillig, M. C. *et al.* The role of multiple global change factors in driving soil functions and
381 microbial biodiversity. *Science* **366**, 886–890 (2019).
- 382 11. Guerra, C. A. *et al.* Global vulnerability of soil ecosystems to erosion. *Landsc. Ecol.* (2020)
383 doi:10.1007/s10980-020-00984-z.

- 384 12. Geisen, S., Wall, D. H. & van der Putten, W. H. Challenges and Opportunities for Soil
385 Biodiversity in the Anthropocene. *Curr. Biol.* **29**, R1036–R1044 (2019).
- 386 13. Jung, M. *et al.* Areas of global importance for conserving terrestrial biodiversity, carbon
387 and water. *Nat Ecol Evol* (2021) doi:10.1038/s41559-021-01528-7.
- 388 14. Xu, H. *et al.* Ensuring effective implementation of the post-2020 global biodiversity targets.
389 *Nat Ecol Evol* **5**, 411–418 (2021).
- 390 15. IPBES. *Summary for policymakers of the global assessment report on biodiversity and*
391 *ecosystem services of the Intergovernmental Science-Policy Platform on Biodiversity and*
392 *Ecosystem Services.* (2019).
- 393 16. Phillips, H. R. P. *et al.* Global distribution of earthworm diversity. *Science* **366**, 480–485
394 (2019).
- 395 17. van den Hoogen, J. *et al.* Soil nematode abundance and functional group composition at
396 a global scale. *Nature* (2019) doi:10.1038/s41586-019-1418-6.
- 397 18. Delgado-baquerizo, M. *et al.* A global atlas of the dominant bacteria found in soil. *Science*
398 **325**, 320–325 (2018).
- 399 19. Tedersoo, L. *et al.* Fungal biogeography. Global diversity and geography of soil fungi.
400 *Science* **346**, 1256688 (2014).
- 401 20. Xu, X., Thornton, P. E. & Post, W. M. A global analysis of soil microbial biomass carbon,
402 nitrogen and phosphorus in terrestrial ecosystems: Global soil microbial biomass C, N
403 and P. *Glob. Ecol. Biogeogr.* **22**, 737–749 (2013).
- 404 21. Djukic, I. *et al.* Early stage litter decomposition across biomes. *Sci. Total Environ.* (2018).
- 405 22. Guerra, C. A. *et al.* Global projections of the soil microbiome in the Anthropocene. *Glob.*
406 *Ecol. Biogeogr.* **30**, 987–999 (2021).
- 407 23. Cameron, E. K. *et al.* Global mismatches in aboveground and belowground biodiversity.
408 *Conserv. Biol.* (2019) doi:10.1111/cobi.13311.
- 409 24. El Moujahid, L. *et al.* Effect of plant diversity on the diversity of soil organic compounds.
410 *PLoS One* **12**, e0170494 (2017).
- 411 25. Guerra, C. A. *et al.* Blind spots in global soil biodiversity and ecosystem function research.
412 *Nat. Commun.* **11**, 3870 (2020).
- 413 26. Fierer, N. & Jackson, R. B. The diversity and biogeography of soil bacterial communities.
414 *Proc. Natl. Acad. Sci. U. S. A.* **103**, 626–631 (2006).
- 415 27. Tedersoo, L. *et al.* Regional-Scale In-Depth Analysis of Soil Fungal Diversity Reveals
416 Strong pH and Plant Species Effects in Northern Europe. *Front. Microbiol.* **11**, 1953
417 (2020).
- 418 28. Popp, A. *et al.* Land-use futures in the shared socio-economic pathways. *Glob. Environ.*
419 *Change* **42**, 331–345 (2017).
- 420 29. Dornelas, M. *et al.* Assemblage Time Series Reveal Biodiversity Change but Not
421 Systematic Loss. *Science* **344**, 296–299 (2014).
- 422 30. Egoh, B., Reyers, B., Rouget, M., Bode, M. & Richardson, D. M. Spatial congruence
423 between biodiversity and ecosystem services in South Africa. *Biol. Conserv.* **142**, 553–
424 562 (2009).
- 425 31. Jürgens, N. *et al.* The BIOTA Biodiversity Observatories in Africa—a standardized
426 framework for large-scale environmental monitoring. *Environ. Monit. Assess.* **184**, 655–
427 678 (2012).
- 428 32. Wyborn, C. & Evans, M. C. Conservation needs to break free from global priority mapping.
429 *Nat Ecol Evol* (2021) doi:10.1038/s41559-021-01540-x.
- 430 33. Hautier, Y. *et al.* Local loss and spatial homogenization of plant diversity reduce
431 ecosystem multifunctionality. *Nat Ecol Evol* **2**, 50–56 (2018).
- 432 34. Zhou, Z., Wang, C. & Luo, Y. Meta-analysis of the impacts of global change factors on
433 soil microbial diversity and functionality. *Nat. Commun.* **11**, 3072 (2020).
- 434 35. Eisenhauer, N., Schulz, W., Scheu, S. & Jousset, A. Niche dimensionality links
435 biodiversity and invasibility of microbial communities. *Funct. Ecol.* **27**, 282–288 (2013).
- 436 36. Wagg, C., Bender, S. F., Widmer, F. & van der Heijden, M. G. A. Soil biodiversity and soil
437 community composition determine ecosystem multifunctionality. *Proc. Natl. Acad. Sci. U.*
438 *S. A.* **111**, 5266–5270 (2014).

- 439 37. Haines-Young, R. H. & Potschin, M. B. The links between biodiversity, ecosystem
440 services and human well-being. in *Ecosystems ecology: a new synthesis* 31 (2009).
441 38. Smith, L. C. *et al.* Large-scale drivers of relationships between soil microbial properties
442 and organic carbon across Europe. *Glob. Ecol. Biogeogr.* **30**, 2070–2083 (2021).
443 39. Keesstra, S. *et al.* The superior effect of nature based solutions in land management for
444 enhancing ecosystem services. *Sci. Total Environ.* **610-611**, 997–1009 (2018).
445 40. Le Provost, G. *et al.* Contrasting responses of above- and belowground diversity to
446 multiple components of land-use intensity. *Nat. Commun.* **12**, 3918 (2021).
447 41. Tanneberger, F. *et al.* The power of nature-based solutions: How peatlands can help us
448 to achieve key EU sustainability objectives. *Adv. Sustain. Syst.* **5**, 2000146 (2021).
449 42. Johnston, A. *et al.* Observed and predicted effects of climate change on species
450 abundance in protected areas. *Nat. Clim. Chang.* **3**, 1055–1061 (2013).
451 43. Hannah, L. *et al.* Protected area needs in a changing climate. *Front. Ecol. Environ.* **5**,
452 131–138 (2007).
453 44. Gallardo, B. *et al.* Protected areas offer refuge from invasive species spreading under
454 climate change. *Glob. Chang. Biol.* **23**, 5331–5343 (2017).
455 45. O'Neill, B. C. *et al.* The roads ahead: Narratives for shared socioeconomic pathways
456 describing world futures in the 21st century. *Glob. Environ. Change* **42**, 169–180 (2017).
457 46. Fedele, G., Donatti, C. I., Bornacelly, I. & Hole, D. G. Nature-dependent people: Mapping
458 human direct use of nature for basic needs across the tropics. *Glob. Environ. Change*
459 102368 (2021).
460 47. Visconti, P. *et al.* Protected area targets post-2020. *Science* **364**, 239–241 (2019).
461 48. Allan, J. R. *et al.* The minimum land area requiring conservation attention to safeguard
462 biodiversity. *Science* **376**, 1094–1101 (2022).
463

464 **List of figures:**

465 **Fig. 1** Current distribution of global soil ecological hotspots. The proportion of land occupied by hotspots
466 of alpha diversity (A), community dissimilarity (B) and ecosystem services (C) (Supplementary Table 2;
467 Extended Data Fig. 4 and 5). The top row corresponds to the proportion of global area occupied by
468 single taxa (A, B) or ecosystem services (C), and the bottom row to the global representation of
469 accumulated hotspots across taxa (A, B) or ecosystem services (C). Together, these three soil
470 ecological dimensions create a soil nature conservation profile where both areas that maximize a given
471 dimension and areas that allow for preserving a combination of global soil biodiversity hotspots are
472 identified (D). Grey areas correspond to areas that were not assessed during calculation due to high
473 uncertainty and insufficient environmental coverage (corresponding to 38.4% of the terrestrial world;
474 Supplementary Figure 5). A further estimation of spatial uncertainty for each dimension considered is
475 given in Supplementary Figures 12 and 13.

476
477 **Fig. 2** Current distribution of the global soil nature conservation priority areas. Spatial representation of
478 the top 5%, 10%, 20%, and 30% areas with the highest accumulation of soil biodiversity and ecosystem
479 services hotspots (A), and the proportion of those areas that are under some form of nature
480 conservation regime (B). Grey areas correspond to areas that were not assessed during calculation.

481

482 **Fig. 3** Expected changes (2015-2070) in the total area of soil nature conservation priorities (top 5%)
483 according to 4 different future shared socio-economic pathways (SSP1, SSP3, SSP4, and SSP5²⁸).

484 ECA: Europe and Central Asia, NMA: North and MesoAmerica, SA: South America, AP: Asia-Pacific,
485 Af: Africa. Light grey areas correspond to areas that were not assessed during calculation.
486
487

488 **Methods**

489

490 ***A global standardized survey to investigate topsoil biodiversity and function***

491 We used composite topsoil samples from global field surveys which were conducted between
492 2016-2019 following standardized field protocols. This global field survey includes 151
493 locations from all continents and 23 countries, from which 615 composite topsoil samples were
494 collected, providing a large representation of all climatic and vegetation biomes in the planet
495 (Supplementary Fig. 1). The locations of the soil samples was not established following a
496 random protocol but rather were selected taking into account the local representativeness of
497 the vegetation within the ecosystem types sampled. In global terms, the approach aimed to
498 include as much climatic and edaphic variability as possible given the constraints of such a
499 sampling scheme. Between three and five composite soil (top ~0-10cm) samples (from 5-10
500 soil cores) were collected in these locations (ranging between 0.09-0.25 ha) following the
501 protocol described in Maestre et al. (2012). By including multiple composite samples within
502 each location, we aimed to account for within-location heterogeneity variation in soil
503 properties, biodiversity and services. We focused on the topsoils, because they are known to
504 hold the largest portion of soil biodiversity, and constitute the critical zone supporting key soil
505 processes from OM decomposition to plant-soil interactions. A portion of these soils was
506 frozen (-20 °C) after sampling for molecular analyses, while another portion was air-dried and
507 used for determining soil properties. We recognize that while our dataset provides a quite
508 complete coverage of global environmental conditions, an increase of sampling locations in
509 less represented regions of the globe would increase the strength of the study. To this respect,
510 we aimed at adequately representing the spatial limitations of our study by eliminating and
511 masking out all the regions that were poorly represented (Supplementary Figure 5). It is also
512 important to mention that reaching this spatial representation is not a trivial endeavor with
513 several logistic limitations (e.g., absence of local resources for sample preservation and
514 consequent material degradation; ²⁵), and overshadowed by war and current transport
515 embargos. These issues disproportionately affect these underrepresented regions and result in
516 important gaps in Africa and South-East Asia. Dataset available here:
517 figshare.com/s/fb33c5a79fcee29e70dc

518 ***Soil biodiversity***

519 The alpha diversity (corresponding to the number of phylotypes) and community dissimilarity
520 (averaged Jaccard distance across samples from presence/absence matrices to account for
521 dissimilarity in phylotypes, measured as ASVs, rather than in their proportions) of archaea,
522 bacteria, fungi, protists and invertebrates was determined using amplicon sequencing
523 technology (Illumina Miseq platform) following the protocol in Delgado-Baquerizo et al. (2019).
524 Both these measurements are critical to understand the nature and conservation potential of
525 specific areas. While alpha diversity refers to the number of species (or ASVs in this case)
526 contained in a particular location, typically seen as priority areas for nature conservation,
527 community dissimilarity refers to the uniqueness of the community, signaling the presence of
528 specific species that are not common elsewhere. The later also represents a critical aspect for
529 the selection of new conservation areas ⁴⁹. Soil DNA was extracted using the Powersoil® DNA
530 Isolation Kit (MoBio Laboratories, Carlsbad, CA, USA) according to the manufacturer's
531 instructions. A portion of the bacterial/archaeal 16S and eukaryotic 18S rRNA genes were
532 sequenced using the 515F/806R and Euk1391f/EukBr primer sets ⁵⁰⁻⁵², respectively.

533 Bioinformatics processing was performed using a combination of QIIME⁵³, USEARCH⁵⁴ and
534 UNOISE3^{55,56}. Phylotypes (i.e. Amplicon sequence variant; ASVs) were identified at the 100%
535 identity level. The ASV abundance tables were rarefied at 5000 (bacteria via 16S rRNA gene),
536 100 (archaea via 16S rRNA gene), 2000 (fungi via 18S rRNA gene), 1000 (protists via 18S
537 rRNA gene), and 250 (invertebrates via 18S rRNA gene) sequences/sample, respectively, to
538 ensure even sampling depth within each belowground group of organisms. Protists are defined
539 as all eukaryotic taxa, except fungi, invertebrates (Metazoa) and vascular plants
540 (Streptophyta). Note that not all samples passed our rarefaction cut-off. The total number of
541 samples included in each soil group is available in Supplementary Table 2.

542 Library preparation and Sequencing

543 Triplicate PCR reactions were performed for each of the extracted DNA samples, and we
544 included and sequenced multiple negative controls per plate to check for possible
545 contamination. Each 25µl PCR reaction contained: 12.5µl of Promega GoTaq Hot Start
546 Colorless Master Mix; 0.5 µl of each barcoded primer (bacterial 16S, 515F [5'-
547 GTGCCAGCMGCCGCGGTAA-3'] and 806R [5'-GGACTACHVGGGTWTCTAAT-3'] OR
548 eukaryotic 18S, Euk1391f (5'-GTACACCGCCCGTC-3') and EukBr (5'-
549 TGATCCTTCTGCAGGTTACCTAC-3'); 10.5 µl water; 1 µl of template DNA. 'Fusion' primers
550 also included Illumina adapters and 12-bp barcodes to enable multiplexed sequencing. PCR
551 conditions for bacterial 16S rDNA amplifications were 94°C for 3min; 35 cycles of 94°C for
552 45s, 50°C for 60s, 72°C for 90s; 72°C for 5 min. PCR conditions for eukaryotic 18S rDNA
553 amplifications were 94°C for 3 min; 35 cycles of 94°C for 45s, 57°C for 60s, 72°C for 90s; 72°C
554 for 10 min. PCR products were cleaned with the MoBio Ultra Clean PCR Clean-Up Kit. Next,
555 we performed PCR-mediated Nextera barcode ligation following the manufacturer's
556 instructions, adding unique barcodes onto amplicons, to allow for multiplexed sequencing.
557 Samples were normalized with the SequelPrep Normalization Plate Kit (Invitrogen) prior to
558 sequencing on the Illumina MiSeq platform.

559 DNA was first cleaned up using AMPure Xp beads (Beckman Coulter, California, USA) and
560 then quantified using the automated fluorescence-based PicoGreen assay (Invitrogen,
561 Massachusetts, USA). The cleaned DNA was normalized to 1.5 ng/µl and a total of 7 ng of the
562 input DNA was used for each amplicon PCR reaction. Illumina's instruction does not
563 recommend pooled three PCRs (which shouldn't be considered as technical replicates), and
564 one PCR reaction was performed per amplicon. While to minimize the PCR bias in the
565 sequencing, the number of PCR cycles was reduced to 25. In detail, the PCR conditions for
566 bacterial 16S rDNA amplification are: 95 °C for 3 min, 25 cycles of 95 °C for 30 sec, 55 °C for
567 30 sec, 72 °C for 30 sec, 72 °C for 5 min then hold at 4 °C; and PCR conditions for eukaryotes
568 18S rDNA amplification is: 94 °C for 5 min, 30 cycles of 94 °C for 30 sec, 55 °C for 30 sec, 72
569 °C for 30 sec, 72 °C for 5 min then hold at 4 °C. The Illumina forward overhang (5'-
570 TCGTCGGCAGCGTCAGATGTGTATAAGAGACAG-3') and reverse overhang (5'-
571 GTCTCGTGGGCTCGGAGATGTGTATAAGAGACAG-3') adapters were included in the
572 amplicon PCR. Each sample was barcoded with two 8 base indices using the Illumina Nextera
573 XT Index Kit. The 15 ul reaction system was prepared with KAPA HotStart ReadyMix Kit
574 (Merck KGaA, Darmstadt, Germany). A ZymoBIOMICS Microbial Community DNA Standard
575 was used as a positive control together with the samples to assess the bias in PCR. Molecular
576 analysis of the full-length ITS region for fungi was performed using ITS9mun/ITS4ngsUni
577 primer sets and PacBio third-generation sequencing as described in⁵⁷. Our sequencing run
578 yielded 3861042 fungal sequences (18s), 534286 invertebrate sequences (18s), 2388020

579 protist sequences (18s), 8901512 bacterial sequences (16s), and 168749 archaeal sequences
580 (16s).

581 Bioinformatics

582 Bioinformatic processing was performed using a combination of QIIME, USEARCH and
583 UNOISE. Briefly, data was demultiplexed and primers were trimmed before further analyses.
584 Default parameters were followed in USEARCH pipeline, except for the bases with a quality
585 score lower than 20 were end-trimmed from the forward/reverse primer reads to minimize the
586 mismatch in merging and to maximize the portion of successful mergers. A maximum of
587 expected error (ee) was set as 1.0 for the merged reads quality filtering using USEARCH
588 (Edgar 2010). zOTUs (or Amplicon Sequence Variant) were gained by denoising (error-
589 correction) the dereplicated merged reads using unoise3 (Edgar 2016). Representative
590 sequences of ASVs were annotated against the Silva database (Quast et al. 2012) in QIIME
591 (Caporaso et al. 2010) using UCLUST⁵⁴. 18S taxonomy annotation used both SILVA and
592 Protist Ribosomal Reference database (PR2, <https://pr2-database.org/>)⁵⁸. Resultant ASV
593 tables were rarefied at 5000 (bacteria via 16S rRNA gene), 100 (archaea via 16S rRNA gene),
594 2000 (fungi via 18S rRNA gene), 1000 (protists via 18S rRNA gene), and 250 (invertebrates
595 via 18S rRNA gene) sequences/sample, respectively, to ensure even sampling depth within
596 each belowground group of organisms. They were then imported into QIIME⁵³ for downstream
597 analysis including diversity and community composition.

598 **Rarefaction resolution and primer set cross-validations**

599 Rarefaction resolution

600 First, we conducted additional analyses to provide evidence that our choice of rarefaction level
601 did not affect our results or conclusions. Here, using the samples with the highest
602 sequence/sample yield, we tested for the impact of different levels of rarefaction on soil
603 biodiversity. We found highly statistically significant correlations between the diversities of soil
604 archaea (rarefied at 100 vs. 500 sequences/sample; Spearman $\rho = 0.764$; $P < 0.001$; $n = 128$),
605 bacteria (rarefied at 5000 vs. 10000 sequences/sample; Spearman $\rho = 0.992$; $P < 0.001$; $n =$
606 509), fungi (rarefied at 2000 vs. 10000 sequences/sample; Spearman $\rho = 0.971$; $P < 0.001$; n
607 $= 88$), protists (rarefied at 1000 vs. 5000 sequences/sample; Spearman $\rho = 0.971$; $P < 0.001$;
608 $n = 287$) and invertebrates (rarefied at 250 vs. 1000 sequences/sample; Spearman $\rho = 0.952$;
609 $P < 0.001$; $n = 274$), for a subset of samples wherein high numbers of sequences were
610 available. These results are supported by previous independent global surveys providing
611 evidence that rarefaction options do not influence global patterns in microbial communities
612^{59,60}. See rarefaction curves in Supplementary Figure 3.

613 Primer set cross-validation

614 Then, we provide additional evidence that primer sets are not influencing the global patterns
615 reported here. For a subset of samples, we generated additional molecular information for
616 fungal (ITS PacBio sequencing; ITS9mun/ITS4ngsUni primer sets) and bacterial (16s rRNA
617 Miseq Sequencing; 341F/805R primer sets) data. We found that the richness soil microbial
618 communities used in this study were highly significantly and positively correlated to those
619 using these alternative primer sets both for bacteria (Spearman $\rho = 0.403$; $P < 0.001$; $n = 128$)
620 and fungi (Spearman $\rho = 0.656$; $P < 0.001$; $n = 228$). Similarly, the community composition of
621 bacteria (Spearman $\rho = 0.479$; $P < 0.001$; $n = 128$) and fungi (Spearman $\rho = 0.414$; $P < 0.001$;

622 n = 228) were significantly and positively correlated to those using these alternative primer
623 sets. More importantly, we also found that the main predictors of bacterial and fungal richness
624 (soil pH in both cases; Supplementary Fig. 2) in this study followed the same pattern for
625 bacterial and fungal richness using alternative primer sets (Supplementary Fig. 4). We would
626 like to further highlight that the 18s primer sets used here to describe protists and invertebrates
627 are the gold standard for the sequencing of these organisms^{52,61} and have been previously
628 cross-validated in the literature^{62–64}. We acknowledge that there are multiple alternative primer
629 sets, especially when specifically targeting particular groups of organisms within protists (e.g.,
630 mtDNA COI gene). Nevertheless, while specific primers may deliver higher resolution for
631 specific groups, these are known to be inefficient in identifying a wide range of organisms from
632 environmental samples⁶⁵.

633 Mapping the distribution of fungal functional guilds

634 Finally, to provide further evidence that 18s rRNA Miseq Sequencing can in this case provide
635 a solid representation of the global patterns in soil-borne mycorrhizal fungi and fungal potential
636 plant pathogens, we compared the global patterns (see mapping method below) in the
637 proportion of soil-borne mycorrhizal fungi and fungal potential plant pathogens determined
638 using 18s rRNA Miseq Sequencing with the subset of data including ITS PacBio sequencing
639 (see above). Our results showed that the proportion of soil-borne mycorrhizal fungi and fungal
640 potential plant pathogens determined using two independent methods followed similar
641 patterns and had a strong and positive correlation worldwide (Supplementary Fig. 6 and Table
642 8 and 9), allowing us to tentatively use the 18S rRNA gene as a proxy for phylotype richness.
643 The number of AMF phylotypes retrieved from ITS PacBio sequencing was not enough to
644 conduct this analysis, so we used Ectomycorrhizal fungi in our mapping comparison.

645 **Soil ecosystem services**

646 Six soil functions directly related to key ecosystem services were determined using highly
647 standardized methods: water retention (water holding capacity), fertility (nitrogen, phosphorus,
648 potassium, and magnesium content), carbon storage (total soil organic carbon content),
649 mutualism (proportion of arbuscular and ectomycorrhizal fungi), pest control (inverse of the
650 proportion of soil-borne potential plant pathogens; as defined here⁶⁶) and OM decomposition
651 (three enzymes associated with C, N and P cycle). Percentage of water holding capacity was
652 determined as in⁶⁷. Soil nitrogen was determined using a CN analyzer. Soil phosphorus,
653 potassium, and magnesium concentrations were determined using ICP (Inductively Coupled
654 Plasma) Spectroscopy after acid digestion⁶⁸. Total soil organic C content was determined
655 from CN analyzer (after removing soil carbonates) and wet-chemistry methods⁵⁹. The
656 proportion of soil-borne fungal potential plant pathogens and fungal plant-soil mutualistic
657 organisms (arbuscular and ectomycorrhizal fungi) were determined as the sum of all taxa
658 classified as such from Funguild⁶⁹ using our 18S dataset. We found Funguild information for
659 297 ASVs of arbuscular mycorrhizal fungi, 217 ASVs of ectomycorrhizal fungi, and 165 ASVs
660 of soil-borne potential fungal plant pathogens. Pest control was calculated as the inverse of
661 the proportion of soil-borne potential plant pathogens (-1 x proportion) as done in⁶⁶. Thus,
662 locations with higher levels of pest control also have lower proportions of plant pathogens. We
663 only focused on those taxa supporting unique trophic life styles. The activity of phosphatase
664 (phosphorus mineralization), beta-glucosidase (starch degradation) and N-acetyl- β -
665 glucosaminidase (chitin degradation) was determined as in⁷⁰ using a high-throughput
666 fluorescence microplate method. The exact number of available information might differ for

667 different ecosystem services (available in Supplementary Table 2). The total number of
668 samples available for each soil attribute is available in Supplementary Table 2. We calculated
669 ecosystem services as the standardized (0-1) average of soil attributes within each ecosystem
670 service (e.g., Fertility: N, P, K and Mg; Mutualism: arbuscular and ectomycorrhizal fungi; OM
671 decomposition: phosphorus mineralization, chitin and starch degradation) using a
672 multifunctionality approach ⁷¹. Furthermore, we acknowledge that the number and type of
673 ecosystem services considered here might be limited to characterize the range of ecological
674 functions driven by soil communities. Therefore, for a subset of the data where other variables
675 are available, we correlated our ecosystem services to additional information on carbon
676 content, enzymes, nutrient availability from IEMS (a proxy of N mineralization; ⁷²) and
677 metagenomics (see Supplementary Table 10).

678 ***Environmental data***

679 Elevation and climatic information for each location was obtained from WorldClim v2 (1 km²
680 resolution; <https://www.worldclim.org/data/bioclim.html>), including information on
681 climatologies and on the seasonality of temperature and precipitation. Soil pH was determined
682 with a soil pH-meter from a soil-water mix ⁷³. Texture was determined as in Maestre et al. ⁷³
683 and, in the case of missing information, this was filled using Soilgrid v2 (<https://soilgrids.org>;
684 as in ¹⁶). Information on dominant vegetation (forest, shrublands or grasslands) was obtained
685 as part of the field survey.

686 ***Drivers of soil biodiversity and services***

687 To investigate the environmental factors associated with soil biodiversity and services, we
688 first used machine learning Random Forest modeling ⁷⁴. We used the R package “rfrpermute”
689 to conduct these analyses. To further strengthen our results, we repeated the same analysis
690 using XGboost algorithms ^{75,76}. XGboost allows for fine-tuning of the model outcomes, and
691 thus results are interesting for answering not only this comment by the reviewer but also the
692 next four comments. In brief, we used a gmtree booster using as an objective function the
693 RMSE using k-fold cross-validation. We tuned the ETA (learning rate), min_chld_weight, max
694 depth, resample, gamma and nfold ⁷⁷ using a Bayesian optimization approach with the
695 package “ParBayesianOptimization” in R ⁷⁸. This allows for efficient implementation of an
696 optimizing search. The parameter we decided to optimize was the test rmse (rather than the
697 train one), in order to prevent overfitting ⁷⁹. The number of trees fitted was also estimated on
698 this criterion using the function xgb.cv from package xgboost in R with 10% of data as
699 validation set. As feature importance, we extracted the gain obtained in predictive, using the
700 function xgb.importance (the results for this second analysis can be found in Supplementary
701 Figure 7; Supplementary Table 11 and 12). Here we chose to train the resulting models using
702 the function xgcv, which fits from 1 to 200 trees to the data and confronts trained models to
703 the cross-validation set. We chose to use the number of trees that minimized the test RMSE.
704 In general, this procedure allows to prevent overfitting (whereas train RMSE might continue
705 being improved, the point where validation RMSE is minimized corresponding to the maximum
706 learning ability without overfitting. In the new analyses, we parameterized 8 important
707 hyperparameters, including the number of trees (nround) and the number of features
708 (colsample_bytree). A full table of the resulting parameters is reported in Supplementary Table
709 11). To further strength our analysis, we compared the results obtained with our approach with
710 results obtained using a GAMM model (considering random factors). GAMMs were performed
711 by flooring coordinates (latitude and longitude) and using their combination as a random factor:

712 ("mdl=gamm(data = ddi,formula =
713 y~s(Latitude)+s(Longitude.cosine)+s(Longitude.sine)+s(s_elev)+Forest+Grassland+Shrubla
714 nd+ s(s_MAT)+s(s_TSEA)+s(s_PSEA)+s(s_MAP)+s(s_SOC)+s(s_Texture)+s(s_pH) random
715 = list(RF=~1)"); being RF the floored combination of latitude and longitude:
716 "dd\$RF=as.factor(paste(floor(coords\$long),floor(coords\$lat)))". This approach allows to
717 control for spatial autocorrelation, apart from the nested structure of our data. Our results show
718 (Supplementary Fig. 10) that the GAMM model provided highly correlated results (Spearman
719 correlations >0.7) for all variables considered and almost identical (very aligned to 1:1 line)
720 predictions to the machine learning algorithms used in our manuscript, suggesting that the
721 type of modelling (e.g., Random Forest vs. GAMM) does not influence our results and
722 conclusions. We also conducted Spearman correlations to better describe the direction of the
723 relationship between environmental factors and soil biodiversity and services. We also
724 correlated all soil biodiversity and services attributes looking for potential trade-offs using
725 Spearman rank correlations. All the analyses in this section are non-parametric, and are
726 especially recommended when dealing with both linear and non-linear relationships. Analyses
727 were done at the sample level to account for within-location variation in soil properties,
728 biodiversity and services.

729 ***Global hotspots of soil biodiversity and services***

730 We used spatially explicit random forest models to predict the distribution of each soil
731 biodiversity and ecosystem service variable. We were able to do these spatial analyses for
732 three main reasons: (1) the high-quality standardized biodiversity and ecosystem service
733 dataset wherein biodiversity and services are measured for the same samples, and analyzed
734 using the same protocols; (2) biodiversity and ecosystem services were highly correlated with
735 key environmental factors at the global scale (Extended Data Figs. 2-3); and (3) the large
736 gradient of environmental conditions in our global dataset covers a large portion (61.6% based
737 on a Mahalanobis analysis) of the large scale environmental variability of the planet. Note that
738 we further spatially constrained our analyses to exclude all environmental outliers^{22,80}.

739 To map each soil biodiversity and ecosystem service variable we used spatially explicit
740 random forest models. For that, we used ArcGIS Pro that estimates random forest models by
741 using an adaptation of the random forest algorithm (a supervised machine learning regression
742 approach) proposed by Breiman et al.^{74,81,82}. Forest-based regressions were trained based
743 on 90% of the dataset, the remaining 10% of the dataset were used for validation purposes.
744 Regression training and validation parameters are given in Supplementary Tables 5 (for Alpha
745 diversity and Community dissimilarity) and 6 (for Ecosystem services). The fitted prediction
746 model was then used to predict the unknown space using a prediction dataset that included
747 all environmental explanatory factors i.e., elevation, carbon, pH, fine texture, mean annual
748 temperature and precipitation, temperature and precipitation seasonality, forest, grassland,
749 shrubland. In the case of the analyses related to the ecosystem services, carbon was excluded
750 from all the models. All models were fitted using 1000 runs for validation and fitting. Prior to
751 prediction all variables included in the dataset and the predictors were resampled to 0.25
752 degrees using an average estimator and scaled. All predictions were made using a 0.25x0.25
753 deg. pixel size. All environmental variables used for spatial projection are listed in
754 Supplementary Table 14.

755 Global hotspots were then calculated using a Getis-Ord G_i^* spatial clustering method⁸³⁻⁸⁵.
756 The Getis-Ord G_i^* statistic was calculated for each location (0.25x0.25 deg. pixel) in the

757 dataset. The resulting z-scores were used to estimate if a given location has statistically high
758 or low values and if these values are spatially clustered. This is done by assessing each
759 location within the context of neighboring locations. Statistically significant positive z-scores
760 indicate clustering of high values (hot spot) and statistically significant negative z-scores the
761 clustering of low values (cold spot). Values for classifying hotspots (positive z-scores) for each
762 variable were taken from the 99% confidence interval. Getis-Ord allows the use of the False
763 Discovery Rate (FDR) correction, which was also applied here, and adjusts the statistical
764 significance of a hot-spot detection to account for multiple testing (with a confidence level of
765 0.95) and spatial dependency⁸⁶. This analysis resulted in a hotspot map for each combination,
766 i.e., five hotspot maps for alpha diversity, five for community dissimilarity, and six for
767 ecosystem services (Extended Data Figs. 4 and 5). We then overlaid the maps for each
768 ecological dimension (i.e., by summing the hotspot maps for each variable in each ecological
769 dimension: alpha diversity, community dissimilarity, and ecosystem services) to obtain a
770 global representation of soil biodiversity hotspots, where a high value corresponds to a
771 concentration of hotspots across multiple taxa or ecosystem services (Fig. 1A, B, and C)

772 ***Spatial uncertainty estimations***

773 One of the difficulties of performing prediction of response variables using a new input dataset
774 is the fact that the new input environmental values might differ substantially from values used
775 to estimate the models. Therefore, estimating uncertainties on the environmental coverage of
776 the datasets as well as the estimations of both biodiversity and ecosystem services is a
777 complex but necessary requirement in such scenario modelling approaches⁸⁷. For this, we
778 have implemented a two-stage approach to tackle both the assessment of the environmental
779 representation of the soil biodiversity and ecosystem services dataset used and the
780 uncertainty related to the estimation of each variable or group of variables. Regarding the first,
781 we calculated the Mahalanobis distance in multidimensional space (here considering the
782 twelve dimensions given by the environmental variables used for modelling (i.e., elevation,
783 carbon, nitrogen, pH, fine texture, mean annual temperature and precipitation, temperature
784 and precipitation seasonality, forest, grassland, shrubland) and centered on the known
785 distribution given by the characteristics, for the same environmental variables, of the soil
786 biodiversity and ecosystem service dataset. This analysis calculates the distance of any point
787 in space to the statistical center, given by the multivariate mean (considering all environmental
788 variables used) of the known distribution. It is often used to detect outliers in point cloud
789 distributions that are assumed to follow a multivariate Normal distribution^{80,88}. The
790 Mahalanobis distance follows a Chi-squared distribution with d degrees of freedom, where d
791 is the dimension of the multidimensional space (d = 12 in our case). Environmental outliers
792 were estimated for a Chi-square of 0.9 (areas in grey in Supplementary Fig. 5).

793 Although this distance is an informative measure of how close a new data point is to the
794 distribution of points in space used to estimate each model, we used a second measure to
795 assess the spatial uncertainty of the estimated values for each model. In order to do this
796 analysis, for each soil biodiversity and ecosystem service variable, we calculated 1000 random
797 iterations of each random forest model and estimated the upper and lower 25% quantile of the
798 distribution of values. We then evaluated uncertainty as the difference between the upper and
799 the lower level of the iteration space for each individual variable. An average representation
800 for each dimension is given in Supplementary Fig. 5.

801 ***Projections of soil biodiversity and ecosystem services under global change scenarios***

802 For the projections of soil biodiversity and ecosystem services, we used the available datasets
803 from the Inter-Sectoral Impact Model Intercomparison Project (ISIMIP)⁸⁹ and from the land-
804 use Model Intercomparison Project (LUMIP)⁹⁰ both activities from the Intergovernmental Panel
805 for Climate Change (IPCC). The selection of scenarios followed the protocol laid out by⁹¹.

806 In terms of climate change projections, we used a bias-corrected future projections dataset for
807 both precipitation and temperature related variables⁸⁹. We considered three Representative
808 Concentration Pathways RCP2.6, RCP6.0, and RCP8.5⁸⁹ with forcing data from three
809 different general circulation models, the IPSL-cm5a-ir, gfdl-esm2m, and noresm1-m⁹². For
810 land-use projections, we used the dataset provided by the land-use Harmonized v2.0 project
811 (<http://luh.umd.edu/>)^{28,93,94}. This dataset was produced in the context of the World Climate
812 Research Program Coupled Model Intercomparison Project 6 (CMIP6)^{28,45,95,96} and contains
813 a harmonized set of land-use scenarios that are consistent between historical reconstructions
814 and future projections. These modeled projections reproduce annual land-use reconstructions
815 for different integrated assessment models (IAMs) and shared socioeconomic pathways (SSP,
816 from 2015 to 2100) at 0.25 degrees resolution, which was developed and widely used to
817 support future biodiversity projections^{97,98}. These shared socioeconomic pathways represent
818 a range of plausible futures based on different socioeconomic challenges for climate change
819 mitigation (low in SSP1 and SSP 4; high in SSP3 and SSP5), and potential challenges for
820 adaptation (low in SSP1 and SSP5; high in SSP3 and SSP4). While full descriptions of these
821 pathways and scenarios are given in²⁸ we provide here a summary of the main characteristics
822 (based on⁴⁵):

823 SSP1: in SSP1 the world shifts gradually, but pervasively, toward a more sustainable path,
824 with its focus on achieving the global development goals, increasing environmental
825 awareness, and a gradual move toward less resource intensive societies. Currently, emerging
826 economies have followed the resource-intensive development model of industrialized
827 countries, but in SSP1, with the focus on equity, and the de-emphasis of economic growth as
828 a goal in high-income countries, leads industrialized countries to support developing countries
829 in their development goals, including green growth strategies, by providing access to human
830 and financial resources and new technologies.

831 SSP3: in SSP3 a resurgent nationalism, concerns about competitiveness and security, and
832 regional conflicts push countries to increasingly focus on domestic or, at most, regional issues.
833 International fragmentation and a world characterized by regional rivalry can already be seen
834 in some of the current regional rivalries and conflicts, but contrasts with globalization trends in
835 other areas. Regional conflict over territorial or national issues produces larger conflicts
836 between major countries, giving rise to increasing antagonism between and within regional
837 blocs, reducing support for international institutions and weakening progress toward the global
838 development goals, particularly in some middle-income countries.

839 SSP4: in SSP4 highly unequal investments in human capital, combined with increasing
840 disparities in economic opportunity and political power, lead to increasing inequalities and
841 stratification both across and within countries. Both across- and within-country inequality is
842 assumed to arise from biased technology development, generally low and highly unequal
843 investments in education resulting in increased restricted access, and reinforced wealth
844 inequality. This pathway assumes that growth is substantially smaller than it is today, but does
845 not assume that it is halted entirely. It also assumes an increased conflict over energy

846 resources between consuming countries and producing countries, particularly if resources are
847 further constrained.

848 SSP5: in SSP5 there is a foreseen acceleration in globalization and rapid development of
849 developing countries. The digital revolution enables an enhanced global discourse which may
850 lead to a rapid rise in global institutions and promote the ability for global coordination. This
851 pathway is driven by the economic success of industrialized and emerging economies to
852 produce rapid technological progress and development of human capital as the path to
853 sustainable development. Global markets are increasingly integrated, with the push for
854 economic and social development coupled with the exploitation of abundant fossil fuel
855 resources and the adoption of resource and energy intensive lifestyles around the world. All
856 these factors lead to rapid growth of the global economy. There is the ability to effectively
857 manage social and ecological systems, including by geo-engineering if necessary. While local
858 environmental impacts are addressed effectively by technological solutions, there is relatively
859 little effort to avoid potential global environmental impacts due to a perceived tradeoff with
860 progress on economic development.

861 All temporal changes (2070 minus 2015, using forecasting predictions) were calculated using
862 2015 as a baseline to which all future predictions were compared.

863

864 **Methods References**

865

- 866 49. Mace, G. M. Whose conservation? *Science* **345**, 1558–1560 (2014).
- 867 50. Amaral-Zettler, L. A., McCliment, E. A., Ducklow, H. W. & Huse, S. M. A method for
868 studying protistan diversity using massively parallel sequencing of V9 hypervariable
869 regions of small-subunit ribosomal RNA genes. *PLoS One* **4**, e6372 (2009).
- 870 51. Stoeck, T. *et al.* Multiple marker parallel tag environmental DNA sequencing reveals a
871 highly complex eukaryotic community in marine anoxic water. *Mol. Ecol.* **19 Suppl 1**, 21–
872 31 (2010).
- 873 52. Ramirez, K. S. *et al.* Biogeographic patterns in below-ground diversity in New York City's
874 Central Park are similar to those observed globally. *Proc. Biol. Sci.* **281**, (2014).
- 875 53. Caporaso, J. G. *et al.* QIIME allows analysis of high-throughput community sequencing
876 data. *Nat. Methods* **7**, 335–336 (2010).
- 877 54. Edgar, R. C. Search and clustering orders of magnitude faster than BLAST.
878 *Bioinformatics* **26**, 2460–2461 (2010).
- 879 55. Edgar, R. C. & Flyvbjerg, H. Error filtering, pair assembly and error correction for next-
880 generation sequencing reads. *Bioinformatics* **31**, 3476–3482 (2015).
- 881 56. Edgar, R. C. UNOISE2: improved error-correction for Illumina 16S and ITS amplicon
882 sequencing. *BioRxiv* (2016).
- 883 57. Tedersoo, L. *et al.* Towards understanding diversity, endemism and global change
884 vulnerability of soil fungi. *bioRxiv* 2022.03.17.484796 (2022)
885 doi:10.1101/2022.03.17.484796.
- 886 58. Quast, C. *et al.* The SILVA ribosomal RNA gene database project: improved data
887 processing and web-based tools. *Nucleic Acids Res.* **41**, D590–6 (2013).
- 888 59. Delgado-Baquerizo, M. *et al.* Changes in belowground biodiversity during ecosystem
889 development. *Proc. Natl. Acad. Sci. U. S. A.* **116**, 6891–6896 (2019).
- 890 60. Delgado-Baquerizo, M. *et al.* Global homogenization of the structure and function in the
891 soil microbiome of urban greenspaces. *Sci Adv* **7**, (2021).
- 892 61. Phillips, H. R. P., Heintz-Buschart, A. & Eisenhauer, N. Putting soil invertebrate diversity
893 on the map. *Mol. Ecol.* **29**, 655–657 (2020).
- 894 62. Xiong, W. *et al.* A global overview of the trophic structure within microbiomes across
895 ecosystems. *Environ. Int.* **151**, 106438 (2021).

- 896 63. Drummond, A. J. *et al.* Evaluating a multigene environmental DNA approach for
897 biodiversity assessment. *Gigascience* **4**, 46 (2015).
- 898 64. Oliverio, A. M., Gan, H., Wickings, K. & Fierer, N. A DNA metabarcoding approach to
899 characterize soil arthropod communities. *Soil Biol. Biochem.* **125**, 37–43 (2018).
- 900 65. Horton, D. J., Kershner, M. W. & Blackwood, C. B. Suitability of PCR primers for
901 characterizing invertebrate communities from soil and leaf litter targeting metazoan 18S
902 ribosomal or cytochrome oxidase I (COI) genes. *Eur. J. Soil Biol.* **80**, 43–48 (2017).
- 903 66. Delgado-Baquerizo, M. *et al.* Multiple elements of soil biodiversity drive ecosystem
904 functions across biomes. *Nat Ecol Evol* **4**, 210–220 (2020).
- 905 67. Carter, M. R. & Gregorich, E. G. *Soil sampling and methods of analysis.* (CRC press,
906 2007).
- 907 68. Sparks, D. L., Page, A. L., Helmke, P. A. & Loeppert, R. H. *Methods of Soil Analysis, Part*
908 *3: Chemical Methods.* (Wiley, 2020).
- 909 69. Nguyen, N. H. *et al.* FUNGuild: An open annotation tool for parsing fungal community
910 datasets by ecological guild. *Fungal Ecol.* **20**, 241–248 (2016).
- 911 70. Bell, C. W. *et al.* High-throughput fluorometric measurement of potential soil extracellular
912 enzyme activities. *J. Vis. Exp.* e50961 (2013).
- 913 71. Wang, L. *et al.* Diversifying livestock promotes multidiversity and multifunctionality in
914 managed grasslands. *Proc. Natl. Acad. Sci. U. S. A.* **116**, 6187–6192 (2019).
- 915 72. Durán, J., Delgado-Baquerizo, M., Rodríguez, A., Covelo, F. & Gallardo, A. Ionic
916 exchange membranes (IEMs): A good indicator of soil inorganic N production. *Soil Biol.*
917 *Biochem.* **57**, 964–968 (2013).
- 918 73. Maestre, F. T. *et al.* Plant species richness and ecosystem multifunctionality in global
919 drylands. *Science* **335**, 214–218 (2012).
- 920 74. Breiman, L. Random Forests. *Mach. Learn.* **45**, 5–32 (2001).
- 921 75. Friedman, J. H. Greedy function approximation: A gradient boosting machine. *aos* **29**,
922 1189–1232 (2001).
- 923 76. Sharma, N. *XGBoost. The Extreme Gradient Boosting for Mining Applications.* (GRIN
924 Verlag, 2018).
- 925 77. Chen, T. & Guestrin, C. XGBoost: A Scalable Tree Boosting System. in *Proceedings of*
926 *the 22nd ACM SIGKDD International Conference on Knowledge Discovery and Data*
927 *Mining 785–794* (Association for Computing Machinery, 2016).
- 928 78. Wilson. ParBayesianOptimization: Parallel Bayesian Optimization of Hyperparameters. *R*
929 *package version 1*, 935 (2021).
- 930 79. Hastie, T., Friedman, J. & Tibshirani, R. The Elements of Statistical Learning. *Springer*
931 *Series in Statistics* (2001) doi:10.1007/978-0-387-21606-5.
- 932 80. Jackson, D. A. & Chen, Y. Robust principal component analysis and outlier detection with
933 ecological data. *Environmetrics* **15**, 129–139 (2004).
- 934 81. Breiman, L. Bagging predictors. *Mach. Learn.* **24**, 123–140 (1996).
- 935 82. Breiman, L., Friedman, J. H., Olshen, R. A. & Stone, C. J. *Classification and regression*
936 *trees.* (Routledge, 2017).
- 937 83. Ord, J. K. & Getis, A. Local spatial autocorrelation statistics: Distributional issues and an
938 application. *Geogr. Anal.* **27**, 286–306 (2010).
- 939 84. Getis, A. & Ord, J. K. The analysis of spatial association by use of distance statistics.
940 *Geogr. Anal.* **24**, 189–206 (2010).
- 941 85. Prasannakumar, V., Vijith, H., Charutha, R. & Geetha, N. Spatio-Temporal Clustering of
942 Road Accidents: GIS Based Analysis and Assessment. *Procedia - Social and Behavioral*
943 *Sciences* **21**, 317–325 (2011).
- 944 86. Lin, G. Comparing spatial clustering tests based on rare to common spatial events.
945 *Comput. Environ. Urban Syst.* **28**, 691–699 (2004).
- 946 87. Araújo, M. B. *et al.* Standards for distribution models in biodiversity assessments. *Sci Adv*
947 **5**, eaat4858 (2019).
- 948 88. Rousseeuw, P. J. & van Zomeren, B. C. Unmasking Multivariate Outliers and Leverage
949 Points. *J. Am. Stat. Assoc.* **85**, 633–639 (1990).
- 950 89. Hempel, S., Frieler, K., Warszawski, L., Schewe, J. & Piontek, F. A trend-preserving bias

- 951 correction – The ISI-MIP approach. *Earth System Dynamics* **4**, 219–236 (2013).
- 952 90. Lawrence, D. M. *et al.* The Land Use Model Intercomparison Project (LUMIP) contribution
953 to CMIP6: rationale and experimental design. *Geoscientific Model Development* vol. 9
954 2973–2998 (2016).
- 955 91. Kim, H. *et al.* A protocol for an intercomparison of biodiversity and ecosystem services
956 models using harmonized land-use and climate scenarios. (2018) doi:10.5194/gmd-11-
957 4537-2018.
- 958 92. Dufresne, J.-L. *et al.* Climate change projections using the IPSL-CM5 Earth System
959 Model: from CMIP3 to CMIP5. *Clim. Dyn.* **40**, 2123–2165 (2013).
- 960 93. Hurtt, G. C. *et al.* Harmonization of land-use scenarios for the period 1500–2100: 600
961 years of global gridded annual land-use transitions, wood harvest, and resulting
962 secondary lands. *Clim. Change* **109**, 117 (2011).
- 963 94. Hurtt, G. C. *et al.* Harmonization of global land use change and management for the
964 period 850–2100 (LUH2) for CMIP6. *Geosci. Model Dev.* **13**, 5425–5464 (2020).
- 965 95. Riahi, K. *et al.* The Shared Socioeconomic Pathways and their energy, land use, and
966 greenhouse gas emissions implications: An overview. *Glob. Environ. Change* **42**, 153–
967 168 (2017).
- 968 96. O'Neill, B. C. *et al.* A new scenario framework for climate change research: the concept
969 of shared socioeconomic pathways. *Climatic Change* vol. 122 387–400 (2014).
- 970 97. Newbold, T. *et al.* Global effects of land use on local terrestrial biodiversity. *Nature* **520**,
971 45–50 (2015).
- 972 98. Powers, R. P. & Jetz, W. Global habitat loss and extinction risk of terrestrial vertebrates
973 under future land-use-change scenarios. *Nat. Clim. Chang.* **9**, 323–329 (2019).

974

975 **Extended Data Figures**

976 **Extended data Fig. 1** Results of Random Forest analysis to identify the main environmental
977 factors associated with soil biodiversity and ecosystem services. Random Forest analyses
978 were done using the rfPermute function of the R package with the same name. MSE = Mean
979 Square Error.

980 **Extended data Fig. 2** Spearman correlations between environmental factors and soil
981 biodiversity and ecosystem services. N in Supplementary Table S1.

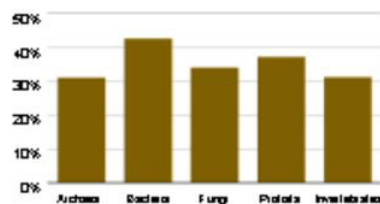
982 **Extended data Fig. 3** Spearman correlations between soil biodiversity and ecosystem
983 services. Total n-values in Supplementary Table S1.

984 **Extended data Fig. 4** Hotspot and coldspot maps for alpha diversity (left) and community
985 dissimilarity (right). The Getis-Ord G_i^* statistic was calculated for each location (0.25x0.25 deg
986 pixel size) in the dataset 1–3. The resulting z-scores were used to estimate if a given location
987 has statistically high or low values and if these values are spatially clustered. This is done by
988 assessing each location within the context of neighboring locations. Statistically significant
989 positive z-scores indicate clustering of high values (hotspot) and statistically significant
990 negative z-scores the clustering of low values (coldspot). Values are plotted for both positive
991 (hotspots) and negative (coldspots) 99%, 95%, and 90% confidence levels.

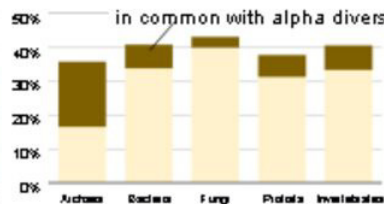
992 **Extended data Fig. 5** Hotspot and coldspot maps for ecosystem services: soil carbon, fertility,
993 OM decomposition, pest control, mutualism, water retention. The Getis-Ord G_i^* statistic was
994 calculated for each location (0.25x0.25 deg pixel size) in the dataset 1–3. The resulting z-
995 scores were used to estimate if a given location has statistically high or low values and if these
996 values are spatially clustered. This is done by assessing each location within the context of
997 neighboring locations. Statistically significant positive z-scores indicate clustering of high
998 values (hotspot) and statistically significant negative z-scores the clustering of low values

999 (coldspot). Values are plotted for both positive (hotspots) and negative (coldspots) 99%, 95%,
1000 and 90% confidence levels.
1001

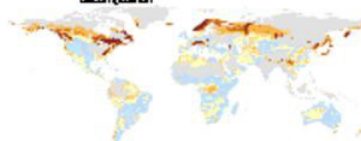
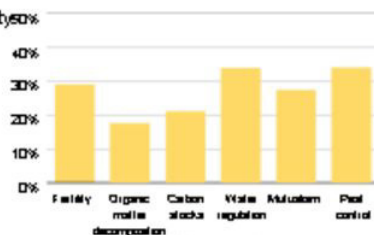
A) Alpha diversity



B) Community dissimilarity



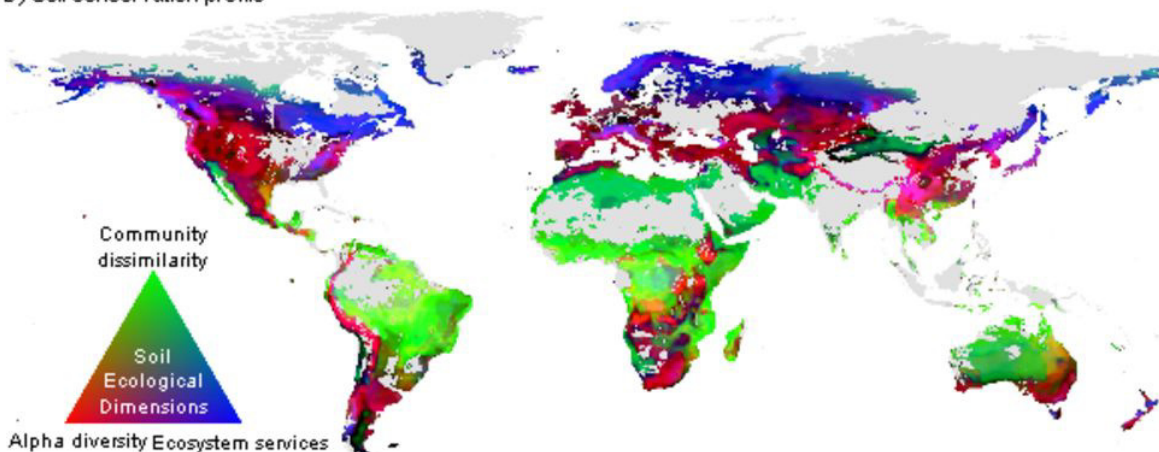
C) Ecosystem services



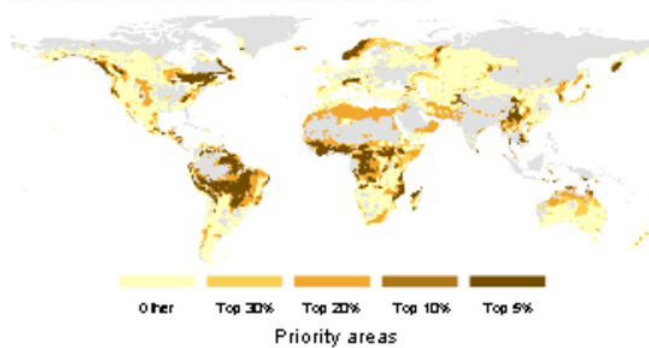
Number of (A,B) taxa or (C) ecosystem service hotspots per pixel



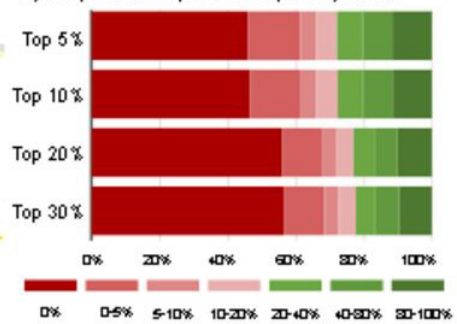
D) Soil conservation profile



A) Global soil nature conservation priorities

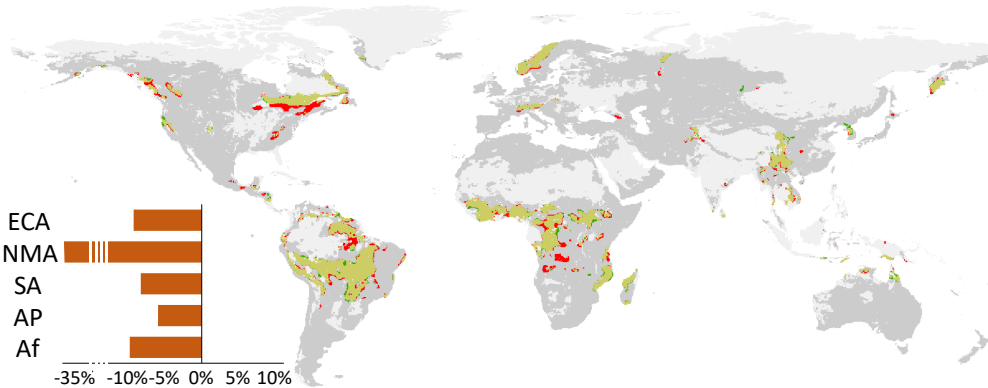


B) Proportion of protected priority areas

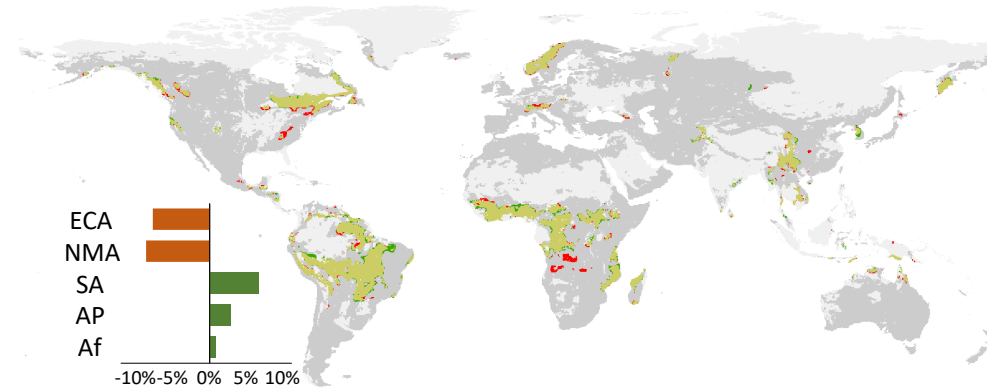


higher challenges for mitigation of impacts

SSP5: Fossil-fueled development

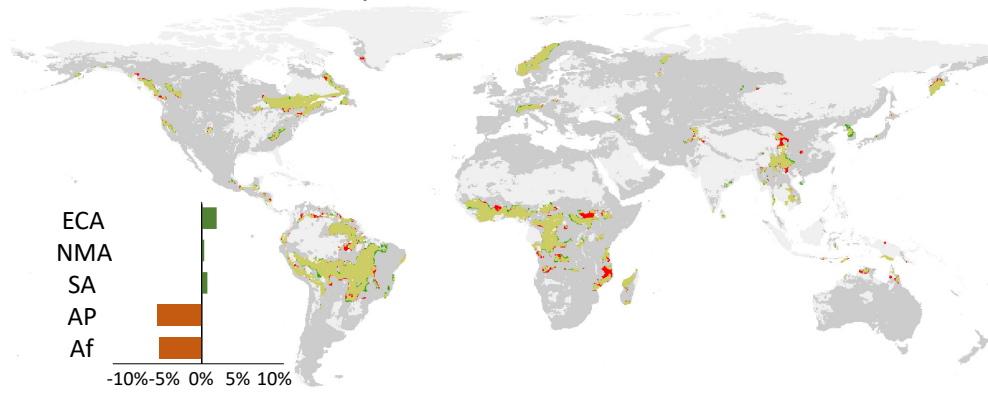


SSP3: Regional rivalry

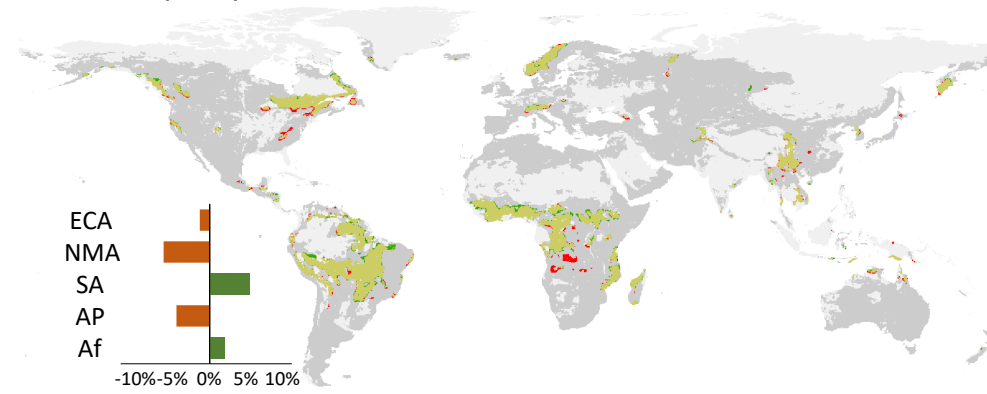


lower challenges for mitigation of impacts

SSP1: Global sustainability



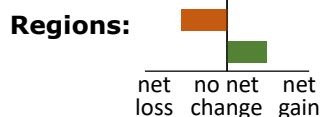
SSP4: Inequality



lower challenges for adaptation to changes in climate

higher challenges for adaptation to changes in climate

- gains (2015-2070) in priority areas
- top 5% priority areas
- losses (2015-2070) in priority areas
- non-priority areas



- ECA: Europe and Central Asia
- NMA: North and Meso America
- SA: South America
- AP: Asia-Pacific
- Af: Africa